SUPPLEMENTARY MATERIAL—Ando *et al.* [Manuscript # 2012-137]

Analytical methods

Planktonic foraminifera

The ooze samples of Site U1348-Core 2R (10 cm-spacing; 15 levels) were weighed for 1.0 g, soaked in 3% H_2O_2 solution for a few hours, gently spray-washed on a 63 µm-opening screen, and oven-dried at <50 °C. To preclude any possibility of carbonate dissolution or mechanical fragmentation through sample processing, water for dilution of H_2O_2 and washing was adjusted to pH = ~10 with a small amount of NH_4OH solution, and an ultrasonic bath not used for cleaning. Each washed sample was dried, sieved on a 125 µm-opening screen, and split accurately using an Otto-splitter if necessary. It was then picked and counted for total foraminifera with *c.* 200–400 individuals of planktonic foraminifera. Identification of planktonic foraminifera was at species-level based on multiple literature sources, in particular Smith & Pessagno (1973), Robaszynski *et al.* (1984), Nederbragt (1991), and Petrizzo *et al.* (2011). Scanning electron microscopic study was performed using a Philips XL-30 ESEM at the National Museum of Natural History, Smithsonian Institution.

Unabbreviated names and IODP sample IDs of specimens in Figure 1 are as follows:

—Interval (i), top-left to clockwise: *Sigalia deflaensis rugocostata* (U1348-2R-CC, 23–24 cm); *Ventilabrella eggeri* (U1348-2R-CC, 10–11 cm); *Hendersonites carinatus* (U1348-2R-CC, 3–4 cm); *Marginotruncana undulata* (U1348-2R-CC, 23–24 cm); *Marginotruncana sinuosa* (U1348-2R-CC, 23–24 cm); *Dicarinella concavata* (U1348-2R-CC, 27–30 cm); *Dicarinella asymetrica* (U1348-2R-CC, 23–24 cm).

—Interval (ii), left to right: *Globotruncanita elevata* (U1348-2R-1, 90–91 cm); *Contusotruncana plummerae* (U1348-2R-1, 91–92 cm).

—Interval (iii), top-left to clockwise: *Globotruncanita stuarti* (U1348-2R-1, 20–21cm); *Globotruncanita subspinosa* (U1348-2R-1, 11–12 cm); *Pseudoguembelina costulata* (U1348-2R-1, 11–12 cm).

—Interval (ii)–(iii), top to bottom: *Globotruncana stephensoni* (U1348-2R-1, 90–91 cm); *Globotruncanita atlantica* (U1348-2R-1, 51–52 cm); *Globotruncana arca* (U1348-2R-1, 90–91 cm); *Globotruncana bulloides* U1348-2R-1, 91–92 cm).

Nannofossils

Calcareous nannofossils were examined in smear slides prepared from raw sediment samples. The slides were observed using standard light microscope techniques, under crossed polarizers, transmitted light, and phase contrast at 1000× magnification. The nannofossil taxonomy and zonation scheme followed Bown

(1998). Taxa were identified down to the species level, and those in poorly preserved assemblages to the genus level.

$CaCO_3$ and total organic carbon (TOC) contents

Relatively small quantities of ooze (*c.* 0.2 g; for economic use of the limited material) were powdered in an agate mortal. Total inorganic carbon (TIC) content was measured using UIC CO_2 coulometer (Model CM5014) at Pusan National University. TIC content was used to calculate $CaCO_3$ content as weight percentage by the multiplication of factor 8.333. The analytical precision of $CaCO_3$ content as relative standard deviation (s.d.) is ±1%. Total carbon (TC) contents were also measured by Flash 2000 Series Elemental Analyzer at Pusan National University. The analytical precision of both parameters are less than ±0.1%. TOC content was calculated by the difference between TC and TIC.

Stable isotopes of bulk carbonates

Bulk stable isotope analysis was carried out at the Bloomsbury Environmental Isotope Facility at University College London. Powdered samples (same set of samples used for $CaCO_3$ and TOC analyses) were first treated with hydrogen peroxide and acetone to oxidize any organic matter, and then analyzed on a ThermoScientific Gas Bench II device connected to a ThermoFinnegan Delta V continuous flow IRMS. Precision of all internal (BDH, IAEA & IFC) and external standards (NBS 19) was ±0.03‰ for $\delta^{13}C$ and ±0.08‰ for $\delta^{18}O$. All values were reported in the Vienna Pee Dee Bee notation (VPDB) after calibration with respect to NBS 19.

Stable Isotopes of Benthic Foraminifera

Several taxon-specific benthic foraminiferal specimens were picked from a narrow size fraction (usually at 212–300 or 180–300 µm but sometimes at 150–180 µm, depending on availability) of washed samples prepared by the same method as planktonic foraminifera. Identification was mainly at genus-level by following Widmark (1997) and also Kaiho (1998), but care was taken so that each separate comprises a single morphotype. The specimens were ultrasonically cleaned in ethanol prior to analysis.

Isotope ratio measurements of the benthic foraminiferal isolates were measured on a ThermoFinnigan™ DeltaPlus mass spectrometer with an on-line automated carbonate reaction Kiel III device at the Biogeochemistry Isotope Laboratory, University of Missouri. Data are reported as per mil (‰) deviation relative on the VPDB scale, and have been normalized among run based on the difference between the within-run average of NBS 19 and its nominal isotopic composition ($\delta^{13}C = -1.95‰$; $\delta^{18}O = 2.20‰$). For standards run with samples that generated >1.5 V of signal for mass 44, replicate measurements of similar-sized NBS 19 ($n = 19$) yielded external precision (1 s.d.) better than ±0.03‰ for

$\delta^{13}C$ and ±0.05‰ for $\delta^{18}O$. In addition, 3 small samples (0.8 to 1.2 V, mass 44) were run with similar-sized standards; those standards (n = 6) ran between 0.7 and 1 V at the precision of ±0.06‰ for $\delta^{13}C$ and ±0.09‰ for $\delta^{18}O$.

Sr isotopes of foraminifera

Foraminiferal tests were hand-picked from the >200 µm washed fraction for Sr isotope analysis. The foraminiferal separates weighing ~150 µg each were briefly sonicated in ethanol followed by purified water, then dissolved using buffered 1M acetic acid (DePaolo *et al.* 1983). Separation of Sr was carried out using Sr Spec cation exchange resin in 100 µL Teflon columns. Sr was loaded in ~2 µL 0.0035M H_3PO_4 on single rhenium filaments between 0.5 µL aliquots of TaF. Isotope ratio measurements were performed on thermal ionization mass spectrometer in the R. Ken Williams Radiogenic Isotope Geosciences Lab at Texas A&M University. The within-run normalization factor for $^{86}Sr/^{88}Sr$ was 0.1194. Replicate measurements of the NIST SRM 987 standard yielded the average of 0.710238 (n = 12), and its difference with respect to the recommended value ($^{87}Sr/^{86}Sr$ = 0.710250 for this study) was used for calibration of all sample $^{87}Sr/^{86}Sr$ data. External reproducibility based on the NIST SRM 987 standard was 9.4 ppm (to 2 s.d.).

Palaeomagnetism

A total of seven discrete sample cubes (2×2×2 cm) were collected from the undisturbed internal portions of the sediment core, and subjected to stepwise alternating field demagnetization. Measurements were performed at the multiple steps (10, 15, 20, 22, 25, 30, 35, 40, 45 and 50 mT) on a 2G Enterprises cryogenic magnetometer installed in a shielded room at the Lamont-Doherty Earth Observatory.

All samples exhibited a clear characteristic component that moves towards the origin of a vector end-point projection (Fig. S3). Three of them showed shallow inclination (two reverse (84.53 and 84.97 mbsf); one normal (85.43 mbsf)), with directions close to that expected for the palaeolatitude of Site U1348 at the time of deposition (~10°N at 80 Ma; Fig. S1). Four other samples (84.43, 84.73, 84.86 and 85.18 mbsf) with reverse polarity showed much steeper inclinations than expected, most likely due to a drilling-induced overprint arising from the rotary core barrel drilling. Note this does not affect the polarity interpretation.

Notes on planktonic foraminiferal biostratigraphy

The Campanian–Maastrichtian biochronology of planktonic foraminifera is complicated by inter-basinal diachroneity of some datum events and should be approached with caution. Such diachroneity has been demonstrated with integrative magnetostratigraphic data even for commonly used zonal biomarkers with distinct keeled morphologies, such as *Abathomphalus mayaroensis* (e.g. Huber & Watkins, 1992) and

Gansserina gansseri (compare Premoli Silva & Sliter (1994) and Li & Keller (1998)). Recently, the middle Campanian *Globotruncana ventricosa* Zone was shown to be unreliable due to significantly site-specific ranges of the nominal index species (Petrizzo *et al.* 2011).

Interval (ii) of Site U1348-Core 2R is assigned to the *G'ta. elevata* (*C. plummerae*) Zone of the early to middle Campanian (Figs. 1, S2). The middle Campanian *C. plummerae* Zone has recently been proposed by Petrizzo *et al.* (2011) in place of the traditional *G. ventricosa* Zone. Its base is defined by the lowest occurrence (LO) of the nominated taxon, which was found to correlate with the lowermost part of Chron C33N in Bottaccione (Italy) and ODP Site 762 (Exmouth Plateau off NW Australia). These authors also presented the similar interpretations without magnetostratigraphy for ODP Hole 1210B (Shatsky Rise) and TDP Site 23 (Tanzania), but the LOs were represented near the bottom of the holes and hence were not highly reliable. In the case of Site U1348, however, *C. plummerae* occurs from interval (ii) having a reversed polarity that is undoubtedly correlated with Chron C33r based on the corresponding Sr isotope ratios (= 0.70756–0.70757). This discrepancy in the magnetochron assignments for the LO of *C. plummerae* is most likely a result of diachroneity in its first appearance datum (FAD), and we infer that the 'true' FAD is slightly older than that proposed by Petrizzo *et al.* (2011). In fact, these authors did not document the evolutionary first appearance of *C. plummerae* with observations of intergradational forms between the ancestral species. As long as the proposed FAD of *C. plummerae* within C33N is based only on the data from two sites without the early evolutionary observations of the nominate species, it is reasonable to assume that its actual FAD still extends back into Chron C33r.

Interval (iii) is somewhat problematic for age interpretation, but the late Campanian age is supported by the co-occurrence of *G'ta. stuarti* and *G'ta. subspinosa* (Robaszynski *et al.* 1984), together with the absence of representative Maastrichtian species. The reversed magnetic interval and Sr isotopic results indicate that this interval should fall within the lower *Globotruncana aegyptiaca* Zone in standard biostratigraphic scheme, but the nominal index species is not present in the Site U1348 assemblage. Interestingly, *G. aegyptiaca* was also reported to be too sporadic to make a reliable zonal assignment in the subtropical western North Atlantic (Huber *et al.* 2008).

Sr isotope stratigraphic ages for central Pacific deep-sea sites

Strategy

The key requirement for this study is objective integration of the new benthic foraminiferal $\delta^{18}O$ data from Site U1348 with published results from DSDP Sites 305 and 463 on the standard numerical time scale. Reliable chronological assessment is particularly essential for the Santonian–Campanian transition interval. In this study Sr isotope stratigraphy provides the primary chronological basis and integration among sites.

Sr isotopes are effective as a chronostratigraphic tool over the intervals where the $^{87}Sr/^{86}Sr$ gradient is relatively steep against time, and the effect of diagenesis is negligible and/or predictable. As discussed below, these conditions generally hold for the sites examined.

Importantly, Sr isotope stratigraphy is advantageous in maintaining the objectivity for the Santonian–Campanian transition chronology of this study. If planktonic foraminiferal datums alone are used for Sites 305 and 463, both sites would necessitate the early–middle Campanian age scaling via extrapolation of age-depth relationship downward from the *Radotruncana calcarata* Zone several tens of meters above, and this treatment would be the source of much uncertainty. Sr isotope stratigraphy also merits in the case of poor core recovery (e.g. Cenomanian–Coniacian interval of Site 463), such that even single $^{87}Sr/^{86}Sr$ data point is convertible to a specific numerical age, with error of <1 m.y. for the Late Cretaceous, whereas microfossil zones inevitably have at least a few million years of resolution. In addition, inter-basinal diachroneity in datum events are present for late Campanian–Maastrichtian planktonic foraminifera (see above Notes on planktonic foraminiferal biostratigraphy).

The following are the basic steps of numerical age assignments for Sites 305 and 463. (1) For each site, the relationship of $^{87}Sr/^{86}Sr$ as a function of sub-bottom depth (i.e. $^{87}Sr/^{86}Sr = f(mbsf)$) is generated using either a linear or polynomial fit to the $^{87}Sr/^{86}Sr$ profile; every level is thus provided a predicted $^{87}Sr/^{86}Sr$ ratio. (2) For the standard Sr isotope curve (modified) (Fig. S4; see next section), the relationship of $^{87}Sr/^{86}Sr$ as a function of age (i.e. $Ma = f(^{87}Sr/^{86}Sr)$) is generated using higher-order polynomials. (3) Substituting the predicted $^{87}Sr/^{86}Sr$ ratio of (1) into $Ma = f(^{87}Sr/^{86}Sr)$ of (2), an age-depth relationship is developed. These procedures are graphically summarized in Figure S5. This is an inverse approach of Ando *et al.* (2009) for Site 463, whose strategy was to plot the Sr isotope data in the standard chronostratigraphic framework using planktonic foraminiferal biochronology. In that study, a good match of the Site 463 Sr isotope data against the reference Sr isotope curves was shown, despite limited planktonic foraminiferal age-controls due to poor core recovery. The present reverse approach should therefore produce a reasonable result as well.

Standard Sr isotope stratigraphy (Fig. S4)

The standard Sr isotope stratigraphy used in this study is from published Late Cretaceous $^{87}Sr/^{86}Sr$ data sources cited in McArthur & Howarth (2004), plotted against the standard magnetobiochronology in GTS2004 of Ogg *et al.* (2004). For compilation of published $^{87}Sr/^{86}Sr$ data, datum levels presented in respective literature sources (upward-pointing arrows in Fig. S4) are updated using GTS2004, and used for rescaling of the $^{87}Sr/^{86}Sr$ data assuming a linear sedimentation rate between adjacent datums. In this study, the Campanian–Maastrichtian portion of McArthur *et al.*'s (1994) data are not adopted because some uncertainties may still exist regarding the correlation of Campanian U.S. Western Interior ammonite zones to the standard geomagnetic polarity time scale (Leahy & Lerbekmo, 1994; Ward *et al.* 2012). Besides, Campanian–Maastrichtian within-biozone $^{87}Sr/^{86}Sr$ variation is somewhat larger, and the $^{87}Sr/^{86}Sr$ ratios are slightly offset when integrated with the European Sr isotope curve. One thing to note is that the range of the planktonic foraminiferal *Rd. calcarata* Zone, an important bioevent for mid-Campanian open-ocean correlation worldwide, is intuitively narrower than usual in GTS2004, although the reason is unclear. An alternative range of the *Rd. calcarata* Zone is shown, which is the relative position of the nominal zone within Chron C33n at Gubbio, Italy (Premoli Silva & Sliter, 1994).

DSDP Site 305 (Fig. S5a)

Campanian–Maastrichtian Sr isotope data for Site 305 are generated by Mearon *et al.* (2003) using barites and ‘carbonates’ (type of carbonate material not specified) and by Barrera *et al.* (1997) and Barrera & Savin (1999) using foraminifera at a much narrower stratigraphic coverage. The barite $^{87}Sr/^{86}Sr$ profile shows a fairly consistent linear trend as a function of sub-bottom depth or age, yet there is a minor but noticeable break in the trend at ~160 mbsf (the junction of Cores17 and 18), which can also be seen in the foraminiferal $^{87}Sr/^{86}Sr$ data of Barrera & Savin (1999, Table Appendix 1 therein). Notably, this break clearly correlates with a concerted jump in $\delta^{13}C$ and $\delta^{18}O$ values of benthic foraminifera *Nuttallides truempyi* (Barrera & Savin, 1999) and bulk carbonates (Voigt *et al.* 2010). These observations support an unconformity at the Core 17/18 boundary, justifying the breaking of Sr isotope-based age model into two segments.

To generate the $^{87}Sr/^{86}Sr$ (barite) vs. sub-bottom depth relationship, a linear regression is applied to data from the Core 18–29 interval. Above the unconformity, the same slope of linear function is fitted over the rest of $^{87}Sr/^{86}Sr$ ratios up-section (n = 5). The resultant age-depth curves suggest ~1.7 m.y. of hiatus during the Maastrichtian (69.3–67.6 Ma).

DSDP Site 463 (Fig. S5b)

Sr isotope stratigraphy for this site was presented in Ando *et al.* (2009) using chiefly bulk carbonates for the entire Upper Cretaceous interval, and by Barrera & Savin (1999) using foraminiferal calcite for the upper Campanian–Maastrichtian. These two data sets match closely and compare well with the reference $^{87}Sr/^{86}Sr$ curves when plotted using planktonic foraminiferal ages.

An important feature of the $^{87}Sr/^{86}Sr$ profile is the major step in values within Site 463-Core 26. In Core 26, a color change occurs at 218.9 mbsf (463-26-3, 140 cm) from pinkish-white (below) to white (above), and the top 10 cm of the pinkish-white chalk interval is burrowed (Ando, unpublished observation at IODP Gulf Coast Repository, May 2011). These observations strongly indicate an unconformity at this level; as expected, planktonic foraminifera show a fundamental assemblage compositional change from the

Coniacian (= *Dicarinella concavata* Zone (upper part, with highly evolved form of *D. concavata*)) to Campanian (= *Globotruncanita elevata* Zone), according to preliminary examination of several washed samples (1 sample per section) through Core 26 by the present author.

Note that Ando *et al.* (2009) also reported that the Site 463 $^{87}Sr/^{86}Sr$ profile for the Albian–Turonian interval has marginal offset toward lower $^{87}Sr/^{86}Sr$ ratios than expected biostratigraphically. This site is typified by having significantly low $^{87}Sr/^{86}Sr$ ratios in interstitial-water at greater sub-bottom depth (Ando *et al.* 2009, Appendix 4 therein). Thus, the observed $^{87}Sr/^{86}Sr$ offset is most likely a result of diagenetic overprinting of interstitial-water Sr isotopic signatures.

To generate the numerical age model, the $^{87}Sr/^{86}Sr$ vs. sub-bottom depth relationship is represented by higher-order polynomials. The upper Cenomanian–Coniacian interval (grey line) is broken into two parts at the $^{87}Sr/^{86}Sr$ inflection of 252.58 mbsf, and they are then shifted by +0.000015 in order to make correction for a diagenetic offset (solid line). This adjustment makes the $^{87}Sr/^{86}Sr$ ratio of the inflection point at Site 463 equivalent to $^{87}Sr/^{86}Sr$ for the correlative 95 Ma $^{87}Sr/^{86}Sr$ inflection baseline in the standard Sr isotope curve. Comparing with the standard $^{87}Sr/^{86}Sr$ curve, the age-depth relationship is proposed for Site 463, which shows that the duration of latest Coniacian–early Campanian hiatus is 6.6 m.y. (86.2–79.6 Ma).

Accuracy of Sr isotope-derived ages

Reliability of the Sr isotope-based chronology described above is supported by: (1) one-by-one correspondence of planktonic foraminiferal zones between Site 463 and GTS2004 via the Sr isotopic age-depth curve through the Cenomanian to mid-Campanian (lack of correlation in the late Campanian–Maastrichtian interval could be due to diachronous planktonic foraminiferal datums); and (2) precise agreement of the $^{87}Sr/^{86}Sr$ ranges for the *Rd. calcarata* Zone between Site 305 ($^{87}Sr/^{86}Sr$ = 0.70767–0.70772 (214.00–186.00 mbsf)) and Site 463 ($^{87}Sr/^{86}Sr$ = 0.70766–0.70770 (192.47–176.71 mbsf)).

References

ANDO, A., NAKANO, T., KAIHO, K., KOBAYASHI, T., KOKADO, E. & KHIM, B.-K. 2009. Onset of seawater $^{87}Sr/^{86}Sr$ excursion prior to Cenomanian–Turonian Oceanic Anoxic Event 2? New Late Cretaceous strontium isotope curve from the central Pacific Ocean. *Journal of Foraminiferal Research*, **39**, 322–334.

BARRERA, E. & SAVIN, S.M. 1999. Evolution of late Campanian–Maastrichtian marine climates and oceans. *In:* Barrera, E. & Johnson, C.C. (eds) *Evolution of the Cretaceous Ocean-Climate System.* Geological Society of America, Special Paper, **332**, 245–282.

BARRERA, E., SAVIN, S.M., THOMAS, E. & JONES, C.E. 1997. Evidence for thermohaline-circulation reversals controlled by sea-level change in the latest Cretaceous. *Geology*, **25**, 715–718.

BOWN, P.R. (ed) 1998. *Calcareous Nannofossil Biostratigraphy*. Kluwer Academic Publishers, Dordrecht, The Netherlands.

CARON, M. 1975. Late Cretaceous planktonic foraminifera from the northwestern Pacific: Leg 32 of the Deep Sea Drilling Project. *In:* Larson, R.L., Moberly, R. *et al. Initial Reports of the Deep Sea Drilling Project*, **32**. U.S. Government Printing Office, Washington, D.C., 719–724.

DEPAOLO, D J., KYTE, F.T., MARSHALL, B.D., O'NEIL, J.R. & SMIT, J. 1983. Rb-Sr, Sm-Nd, K-Ca, O, and H isotopic study of Cretaceous-Tertiary boundary sediments, Caravaca, Spain: evidence for an oceanic impact site. *Earth and Planetary Science Letters,* **64**, 356–373.

EXPEDITION 324 SCIENTISTS. 2010. Site U1348. *In:* Sager, W.W., Sano, T., Geldmacher, J. & the Expedition 324 Scientists. *Proceedings of the Integrated Ocean Drilling Program,* **324**. Integrated Ocean Drilling Program Management International, Inc., Tokyo, doi:10.2204/iodp.proc.324.105.2010.

FRIEDRICH, O., SCHMIEDL, G. & ERLENKEUSER, H. 2006. Stable isotope composition of Late Cretaceous benthic foraminifera from the southern South Atlantic: Biological and environmental effects. *Marine Micropaleontology*, **58**, 135–157.

FRIEDRICH, O., NORRIS, R.D. & ERBACHER, J. 2012. Evolution of middle to Late Cretaceous oceans—A 55 m.y. record of Earth's temperature and carbon cycle. *Geology*, **40**, 107–110.

HUBER, B.T. & WATKINS, D.K. 1992, Biogeography of Campanian-Maastrichtian calcareous plankton in the region of the Southern Ocean: paleogeographic and paleoclimatic implications. *In:* Kennett, J.P. & Warnke, D.A. (eds) *The Antarctic Paleoenvironment: A Perspective on Global Change, Antarctic Research Series*, **56**. American Geophysical Union, Washington, D.C., 31–60.

HUBER, B.T., MACLEOD, K.G. & TUR, N.A. 2008. Chronostratigraphic framework for upper Campanian-Maastrichtian sediments on the Blake Nose (subtropical North Atlantic). *Journal of Foraminiferal Research*, **38**, 162–182.

KAIHO, K. 1998. Phylogeny of deep-sea calcareous trochospiral benthic foraminifera: evolution and diversification. *Micropaleontology*, **44**, 291–311.

LEAHY, G.D. & LERBEKMO, J.F. 1994. Macrofossil magnetobiostratigraphy for the upper Santonian–lower Campanian interval in the Western Interior of North America: comparisons with European stage boundaries and planktonic foraminiferal zonal boundaries. *Canadian Journal of Earth Sciences*, **32**, 247–260.

LI, L. & KELLER, G. 1998. Maastrichtian climate, productivity and faunal turnovers in planktic foraminifera in South Atlantic DSDP sites 525A and 21. *Marine Micropaleontology*, **33**, 55–86.

MCARTHUR, J.M. & HOWARTH, R.J. 2004. Strontium isotope stratigraphy. *In:* Gradstein, F.M., Ogg, J.G. & Smith, A.G. (eds) *A Geologic Time Scale 2004.* Cambridge University Press, Cambridge, 96–105.

MCARTHUR, J.M., THIRLWALL, M.F., CHEN, M., GALE, A.S. & KENNEDY, W.J. 1993a. Strontium isotope stratigraphy in the late Cretaceous: Numerical calibration of the Sr isotope curve and intercontinental correlation for the Campanian. *Paleoceanography*, **8**, 859–873.

MCARTHUR, J.M., THIRLWALL, M.F., GALE, A.S., KENNEDY, W.J., Burnett, J.A., Mattey, D. & LORD, A.R. 1993b. Strontium isotope stratigraphy for the Late Cretaceous: a new curve, based on the English chalk. *In:* Hailwood, E.A. & Kidd, R.B. (eds) *High Resolution Stratigraphy.* Geological Society Special Publication, **70**, 195–209.

MCARTHUR, J.M., KENNEDY, W.J., CHEN, M., THIRLWALL, M.F. & GALE, A.S. 1994. Strontium isotope stratigraphy for Late Cretaceous time: Direct numerical calibration of the Sr isotope curve based on the US Western Interior. *Palaeogeography, Palaeoclimatology, Palaeoecology*, **108**, 95–119.

MEARON, S., PAYTAN, A. & BRALOWER, T.J. 2003. Cretaceous strontium isotope stratigraphy using marine barite. *Geology*, **31**, 15–18.

NEDERBRAGT, A.J. 1991. Late Cretaceous biostratigraphy and development of Heterohelicidae (planktic foraminifera). *Micropaleontology*, **37**, 329–372.

OGG, J.G., AGTERBERG, F.P. & GRADSTEIN, F.M. 2004. The Cretaceous Period. *In:* Gradstein, F.M., Ogg, J.G. & Smith, A.G. (eds) *A Geologic Time Scale 2004.* Cambridge University Press, Cambridge, 344–383.

PETRIZZO, M.R., FALZONI, F. & PREMOLI SILVA, I. 2011. Identification of the base of the lower-to-middle Campanian *Globotruncana ventricosa* Zone: Comments on reliability and global correlations. *Cretaceous Research*, **32**, 387–405.

PREMOLI SILVA, I. & SLITER, W.V. 1994. Cretaceous planktonic foraminiferal biostratigraphy and evolutionary trends from the Bottaccione section, Gubbio, Italy. *Palaeontographia Italica*, **82**, 1–89.

ROBASZYNSKI, F., CARON, M., GONZALES DONOSO, J. M., WONDERS, A.A.H. & THE EUROPEAN WORKING GROUP ON PLANKTONIC FORAMINIFERA. 1984. Atlas of Late Cretaceous globotruncanids. *Revue de Micropaléontologie*, **26**, 145–305.

SAGER, W.W., EVANS, H.F. & CHANNELL, J.E.T. 2005. Paleomagnetism of Early Cretaceous (Berriasian) sedimentary rocks, Hole 1213B, Shatsky Rise. *In:* Bralower, T.J., Premoli Silva, I. & Malone, M.J. (eds) *Proceedings of the Ocean Drilling Program, Scientific Results*, **198**. Ocean Drilling Program, College Station, Texas, doi: 10.2973/odp.proc.sr.198.117.2005.

SHIPBOARD SCIENTIFIC PARTY. 2002. Leg 198 summary. *In:* Bralower, T.J., Premoli Silva, I., Malone, M.J., *et al.*, *Proceedings of the Ocean Drilling Program, Initial Reports*, **198**. Ocean Drilling Program, College Station, Texas, 1–148, doi: 10.2973/odp.proc.ir.198.101.2002.

SMITH, C.C. & PESSAGNO, E.A. 1973, Planktonic foraminifera and stratigraphy of the Corsicana Formation (Maestrichtian) North-Central Texas. Cushman Foundation for Foraminiferal Research, Special Publication, **12**.

SUGARMAN, P.J., MILLER, K.G., BURKY, D. & FEIGENSON, M.D. 1995. Uppermost Campanian–Maestrichtian strontium isotopic, biostratigraphic, and sequence stratigraphic framework of the New Jersey Coastal Plain. *Geological Society of America Bulletin*, **107**, 19–37.

VOIGT, S., FRIEDRICH, O., NORRIS, R.D. & SCHÖNFELD, J. 2010. Campanian – Maastrichtian carbon isotope stratigraphy: shelf-ocean correlation between the European shelf sea and the tropical Pacific Ocean. *Newsletters on Stratigraphy*, **44**, 57–72.

WARD, P.D., HAGGART, J.W., MITCHELL, R., KIRSCHVINK, J.L. & TOBIN, T. 2012. Integration of macrofossil biostratigraphy and magnetostratigraphy for the Pacific Coast Upper Cretaceous (Campanian–Maastrichtian) of North America and implications for correlation with the Western Interior and Tethys. *Geological Society of America Bulletin*, **124**, 957–974.

WIDMARK, J.G.V. 1997. Deep-sea benthic foraminifera from Cretaceous–Paleogene boundary strata in the South Atlantic – taxonomy and paleoecology. *Fossils and Strata*, **43**.

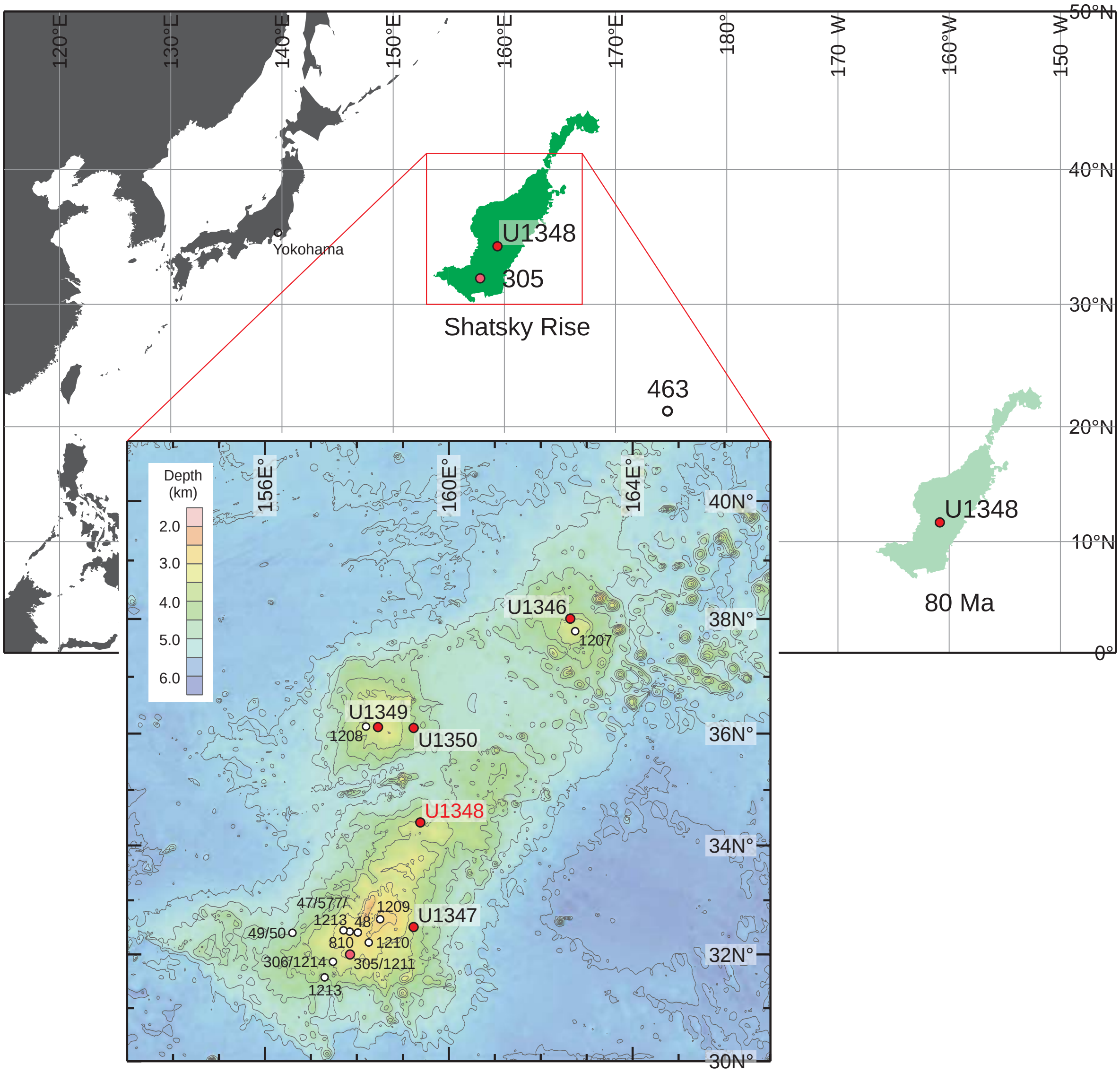

Fig. S1. Map showing present-day locations of IODP Site U1348 (Shatsky Rise), DSDP Site 305 (Shatsky Rise), and DSDP Site 463 (Mid-Pacific Mountains), and color bathymetric map showing all Shatsky Rise DSDP/ODP/IODP sites (courtesy of Will Sager). Also shown is 80 Ma palaeolocation of Shatsky Rise, adopted from Shipboard Scientific Party (2002; Fig. F4 therein). This study follows palaeolatitude reconstruction by Shipboard Scientific Party (2002), which indicates north-of-equator position of Shatsky Rise since the earliest Cretaceous. This estimate is supported by actual palaeomagnetic measurements of Berriasian sediments at Site 1213 (~5°N at ~140 Ma) (Sager *et al.* 2005).

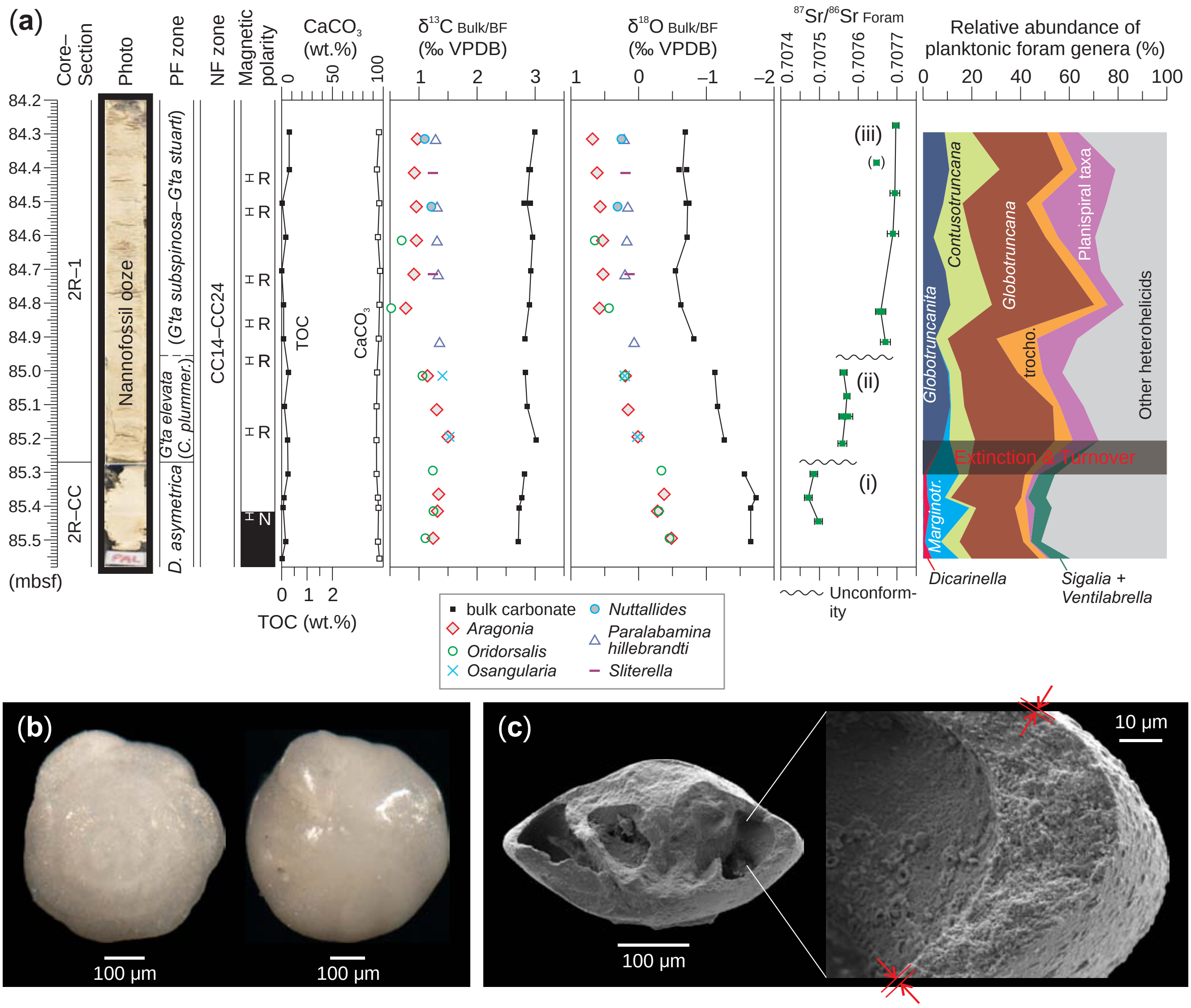

Fig. S2. (**a**) Supplement to Figure 1(main text) with additional diagrams of total organic carbon (TOC) contents, δ^{13}C values of bulk carbonates, and relative abundance of planktonic foraminiferal genera for Site U1348-Core 2R. *Marginotr.*—*Marginotruncana*; trocho.—other trochospiral taxa. Benthic foraminiferal δ ^{18}O values shown are raw data that are not corrected for vital effect-induced inter-taxon offset. (**b**) Stereomicroscopic images of benthic foraminifera showing very good preservation with dully translucent 'pearly' tests: (left) spiral view of *Nuttallides* (IODP Sample U1348-2R-1, 21–22 cm); (right) umbilical view of *Oridorsalis* (IODP Sample U1348-2R-1, 91–92 cm). Dryness of specimens was confirmed before imaging, and hence the demonstrated test translucency and surface reflection are the original features, not because of moistening. (**c**) SEM images of wall cross-section of *Oridorsalis* (IODP Sample U1348-2R-1, 61–62 cm) showing original granular texture. Faint *c.* 1 micron-thick layer of surface dissolution and/or recrystallization can be seen both externally and internally (indicated by paired red arrows).

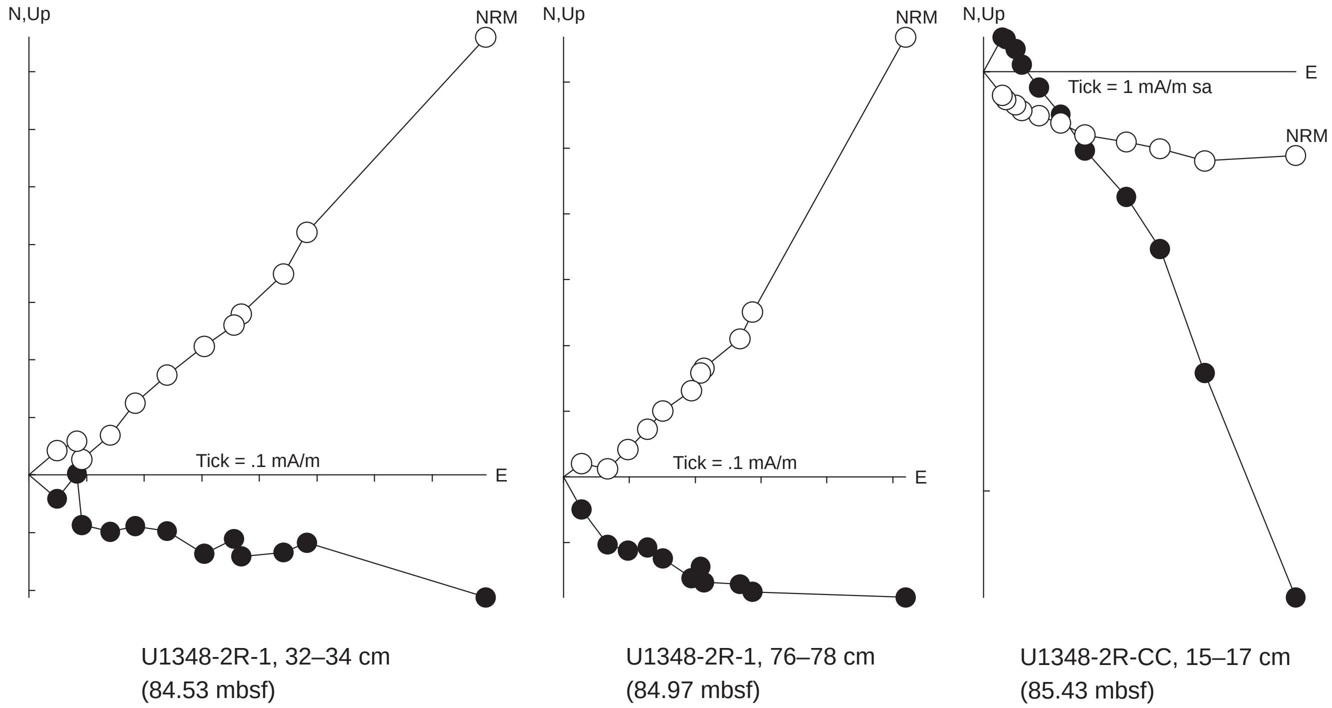

Fig. S3. Examples of orthogonal projections of palaeomagnetic data from Site U1348-Core 2R. Open circles represent vector end point projection on vertical plane (inclination), and closed circles represent vector end point projection on horizontal plane (declination).

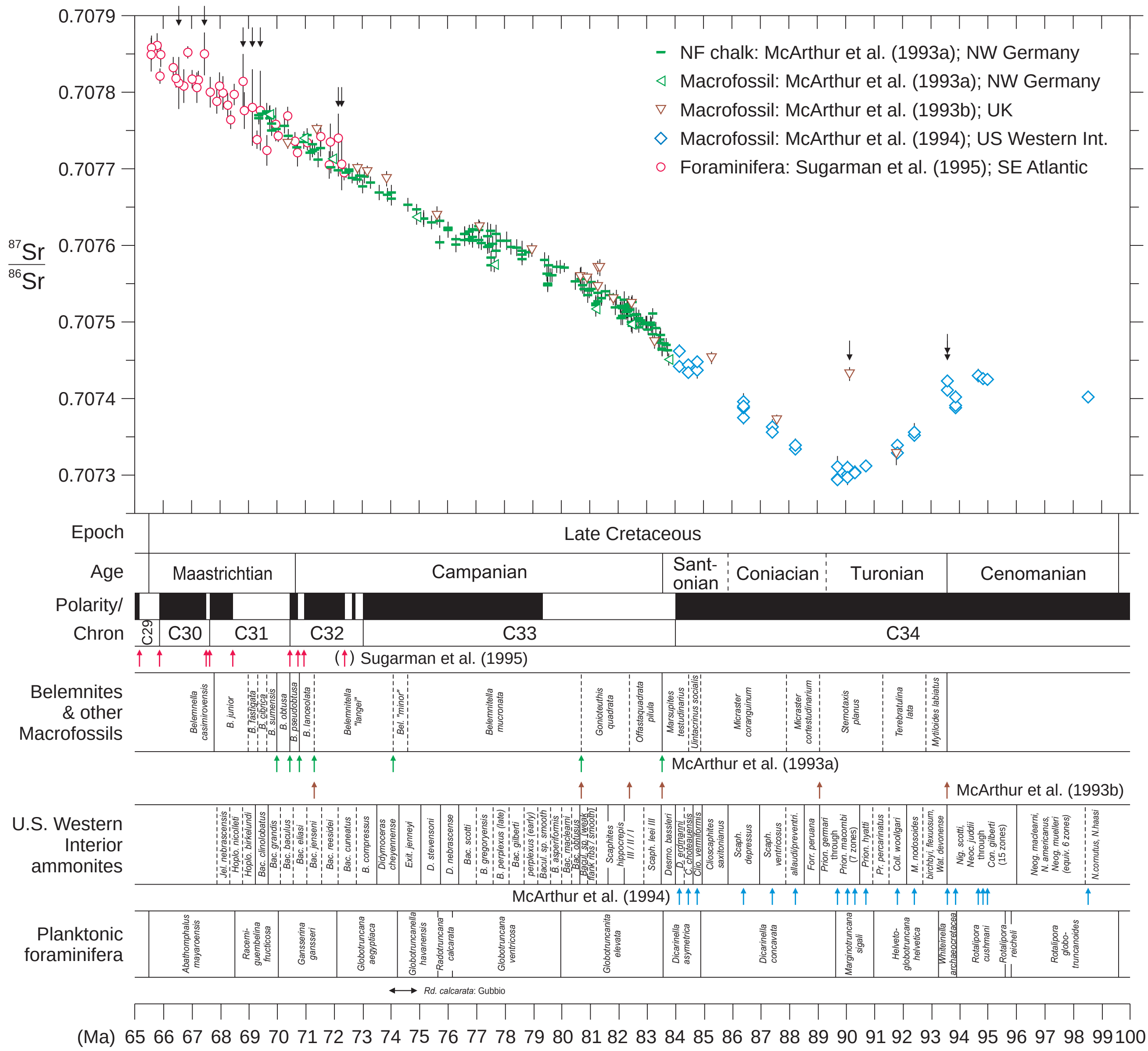

Fig. S4. Compilation of published $^{87}Sr/^{86}Sr$ datasets for standard Late Cretaceous Sr isotope stratigraphy adopted in this study: McArthur *et al.* (1993a), Lägerdorf/Kronsmoor, NW Germany; McArthur *et al.* (1993b), Trunch, UK; McArthur *et al.* (1994), U.S. Western Interior; and Sugarman *et al.* (1995), DSDP Hole 525A, SE Atlantic. All $^{87}Sr/^{86}Sr$ data are recalibrated using NIST SRM 987 = 0.710250, and plotted against GTS2004 using datum levels (upward-pointing arrows) presented in respective literature sources (McArthur *et al.* 1993a, Table 2; McArthur *et al.* 1993b, p. 199, Fig. 2; McArthur *et al.* 1994, Table 1; Sugarman *et al.* 1995, Table 1). Data from McArthur *et al.* (1994) are rescaled using revised mid-point numerical ages of U.S. Western Interior ammonite zones (Ogg *et al.* 2004, Table 19.3 therein). Error bar for each data point is internal precision (±2 standard error). Small black arrows in $^{87}Sr/^{86}Sr$ panel indicate data points not used for regression analysis (Fig. S5c). For Sugarman *et al.* (1995), data with errors greater than ±0.000025 are eliminated. '*Rd. calcarata*: Gubbio' is alternative age range of planktonic foraminiferal *Radotruncana calcarata* Zone based on its relative position in Chron 33n at Gubbio, Italy (Premoli Silva & Sliter 1994).

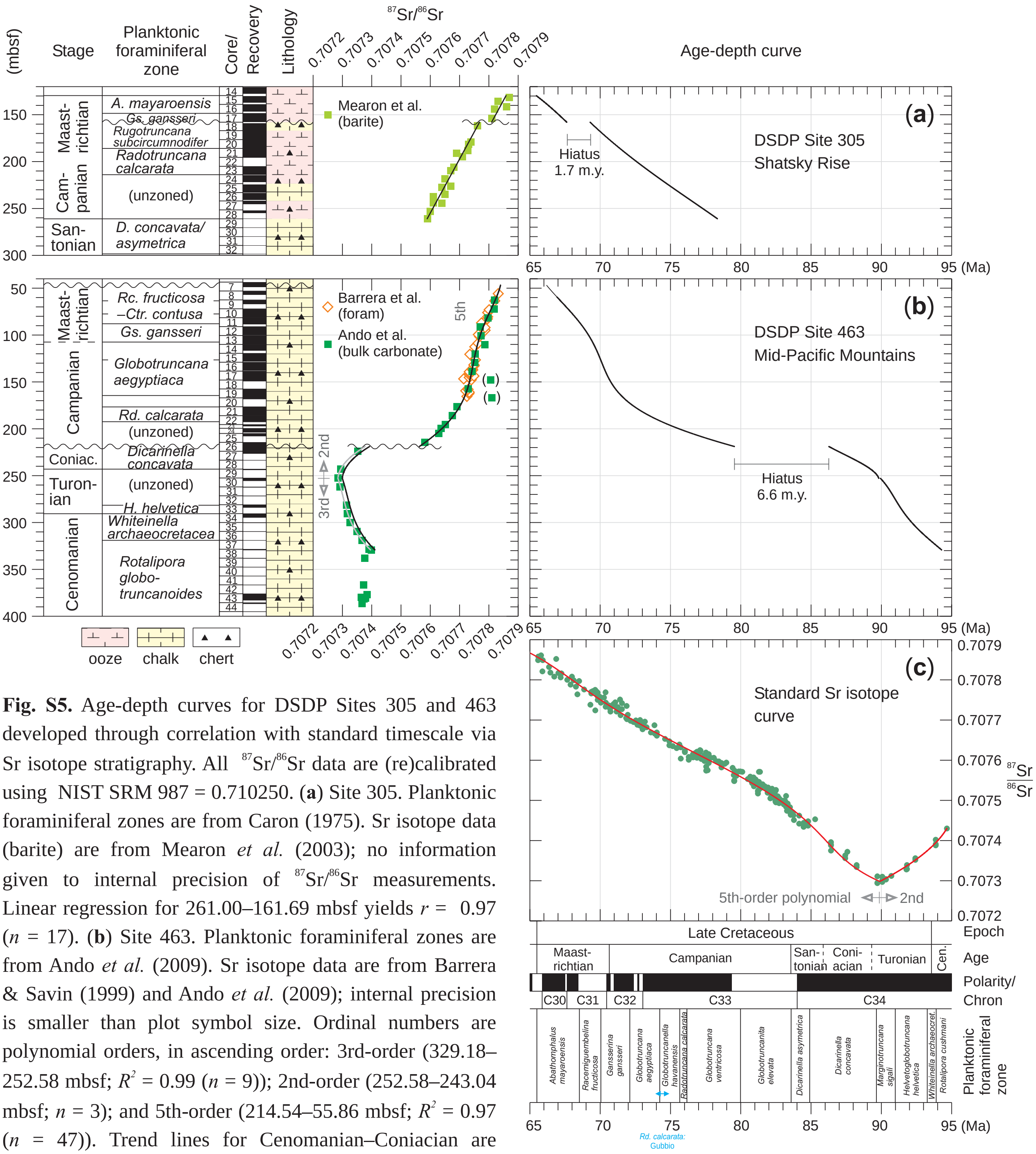

Fig. S5. Age-depth curves for DSDP Sites 305 and 463 developed through correlation with standard timescale via Sr isotope stratigraphy. All $^{87}Sr/^{86}Sr$ data are (re)calibrated using NIST SRM 987 = 0.710250. (**a**) Site 305. Planktonic foraminiferal zones are from Caron (1975). Sr isotope data (barite) are from Mearon *et al.* (2003); no information given to internal precision of $^{87}Sr/^{86}Sr$ measurements. Linear regression for 261.00–161.69 mbsf yields r = 0.97 (n = 17). (**b**) Site 463. Planktonic foraminiferal zones are from Ando *et al.* (2009). Sr isotope data are from Barrera & Savin (1999) and Ando *et al.* (2009); internal precision is smaller than plot symbol size. Ordinal numbers are polynomial orders, in ascending order: 3rd-order (329.18–252.58 mbsf; R^2 = 0.99 (n = 9)); 2nd-order (252.58–243.04 mbsf; n = 3); and 5th-order (214.54–55.86 mbsf; R^2 = 0.97 (n = 47)). Trend lines for Cenomanian–Coniacian are shifted by +0.000015 from original (grey line), in order to maximally compare them with standard Sr isotope curve. Two outliers of $^{87}Sr/^{86}Sr$ in Campanian interval (bracketed), generated from very chert-rich samples, are eliminated as they are presumably from drilling-induced down-hole contaminants. (**c**) Standard Sr isotope curve calibrated against GTS2004 for providing numerical age scales of Sites 305 and 463, adopted from Figure S4. Trend lines are polynomial regressions at 2nd-order (94.66–89.71 Ma; R^2 = 0.97 (n = 18)) and 5th-order (89.71–65.58 Ma; R^2 = 0.99 (n = 220)).

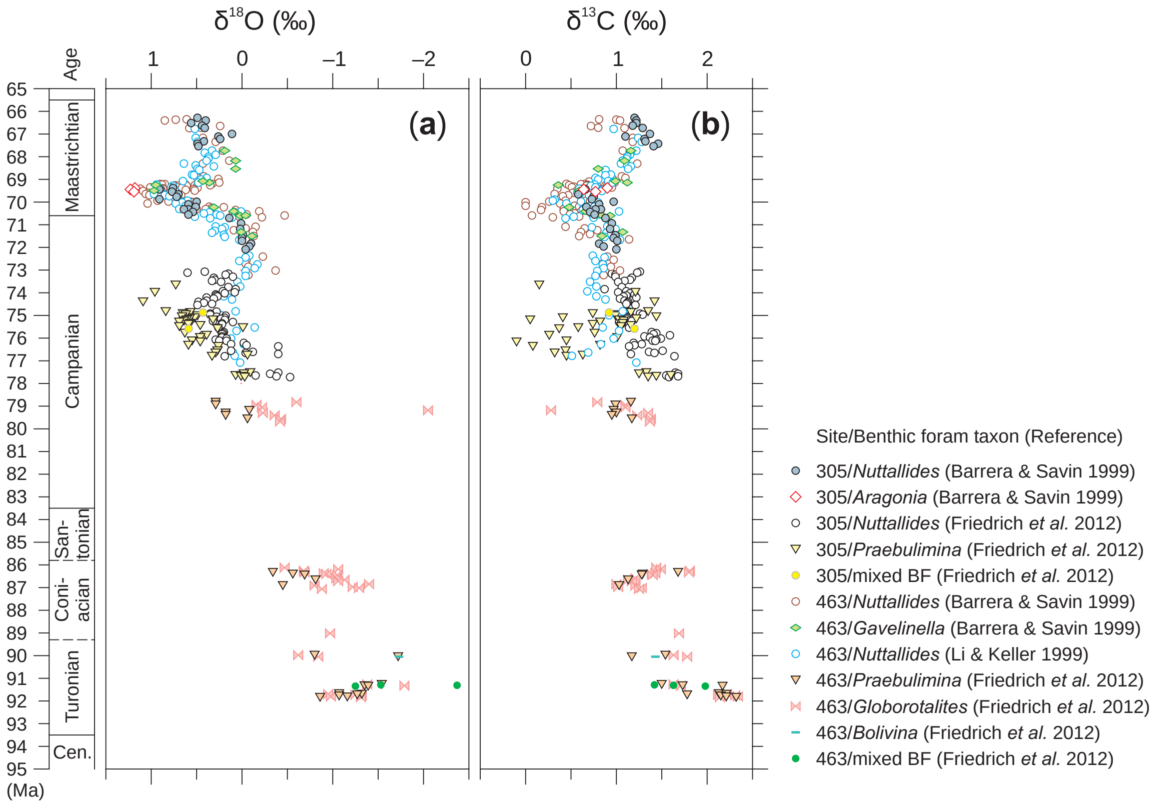

Fig. S6. Updated Late Cretaceous benthic foraminiferal stable isotope compilation for central Pacific DSDP Sites 305 and 463, using age-depth relationships of Figure S5. (**a**) Benthic foraminiferal $\delta^{18}O$ compilation, wit no correction for inter-taxon $\delta^{18}O$ vital effect. Note obvious offset of datasets between *Praebulimina* and *Globorotalites* at Turonian–early Campanian of Site 463 (Friedrich *et al.* 2012). Data points from the latter group are not adopted in Figure 2 (main text); *Globorotalites* shows somewhat extreme isotopic behavior with greater extent of scatter, and it is also known for its disequilibrium $\delta^{18}O$ precipitation (Friedrich *et al.* 2006). (**b**) Benthic foraminiferal $\delta^{13}C$ compilation. Note fairly good match of *Nuttallides* $\delta^{13}C$ values between Sites 305 and 463, providing supportive evidence for the presence of unconformity at Site 305, as illustrated in Figure S5.

TABLE S1. SELECTED PLANKTONIC FORAMINIFERAL OCCURRENCE AND ABUNDANCE, IODP SITE U1348

Sample ID	Depth: mid-point (mbsf)	Zone	*Dicarinella asymetrica*	*Dicarinella concavata*	*Marginotruncana undulata*	*Marginotruncana sinuosa*	*Contusotruncana fornicata*	*Contusotruncana plummerae*	*Contusotruncana patelliformis*	*Globotruncana linneiana* group	*Globotruncana arca*	*Globotruncana bulloides*	*Globotruncana stephensoni*	*Globotruncana hilli*	*Globotruncanita elevata/ stuartiformis*†	*Globotruncanita atlantica*	*Globotruncanita stuartiformis*	*Globotruncanita subspinosa*	*Globotruncanita stuarti*	"*Hedbergella*" *holmdelensis*	*Sigalia rugocostata*	*Ventilabrella eggeri*	*Pseudotextularia nuttalli*	*Hendersonites carinatus*	*Heterohelix planata*	*Pseudoguembelina costulata*	*Pseudoguembelina costellifera*
U1348A-2R-1, 9–10 cm	84.295	(*G'ta subspinosa* —*G'ta stuarti*)*	—	—	—	—	C	—	—	C	R	—	C	—	—	—	F	—	R	R	—	—	—	—	—	F	A
U1348A-2R-1, 20–21 cm	84.405		—	—	—	—	C	—	R	C	R	—	C	—	—	T	F	—	R	R	—	—	—	T	—	F	F
U1348A-2R-1, 30–31 cm	84.505		—	—	—	—	F	—	T	C	R	T	C	—	—	T	F	T	—	R	—	—	—	—	—	F	F
U1348A-2R-1, 40–41 cm	84.605		—	—	—	—	C	—	—	C	R	T	C	—	—	T	R	—	—	R	—	—	—	—	—	F	C
U1348A-2R-1, 50–51 cm	84.705		—	—	—	—	C	—	T	A	R	R	C	—	—	—	F	T	—	R	—	—	—	—	—	F	C
U1348A-2R-1, 60–61 cm	84.805		—	—	—	—	C	—	R	A	R	R	C	—	—	R	F	—	—	—	—	—	T	—	—	—	R
U1348A-2R-1, 70–71 cm	84.905		—	—	—	—	R	R	T	F	R	R	R	—	—	T	R	—	—	T	—	—	—	T	—	T	R
U1348A-2R-1, 80–81 cm	85.005	*G'ta elevata* (*C. plummerae*)	—	—	—	T	R	R	T	C	R	F	T	R	F	R	—	—	—	—	—	—	R	—	—	—	—
U1348A-2R-1, 90–91 cm	85.105		—	—	—	T	R	R	—	C	R	F	T	C	C	T	—	—	—	—	—	—	R	R	—	—	—
U1348A-2R-1, 100–101 cm	85.205		—	—	—	R	F	F	T	C	R	F	T	F	F	R	—	—	—	—	—	—	R	R	—	—	—
U1348A-2R-CC, 3–4 cm	85.305	*Dicarinella asymetrica*	T	T	T	C	R	—	—	C	—	—	—	—	T	—	—	—	—	—	R	R	T	T	R	—	—
U1348A-2R-CC, 10–11 cm	85.375		T	R	—	F	R	—	—	A	—	—	—	—	—	—	—	—	—	—	F	R	T	T	R	—	—
U1348A-2R-CC, 13–14 cm	85.405		R	R	T	C	R	—	—	C	—	—	—	—	T	—	—	—	—	—	R	R	—	—	R	—	—
U1348A-2R-CC, 23–24 cm	85.505		T	T	R	R	F	—	—	A	—	—	—	—	—	—	—	—	—	—	R	T	—	T	—	—	—
U1348A-2R-CC, 27–30 cm	85.555		R	R	T	C	F	—	—	A	—	—	—	—	T	—	—	—	—	—	F	R	T	—	—	—	—

A = abundant (>20%)

C = common (>10–20%)

F = few (>5–10%)

R = rare (>1–5%)

T = trace (≤1%)

— = absent

*Tentatively used as assemblage zone

†High-degree of intergradation seen between two species categories

TABLE S2. SELECTED NANNOFOSSIL OCCURRENCE AND ABUNDANCE, IODP SITE U1348

Sample ID	Depth (mbsf)	*Arkhangsiella confusa*	*Arkhangsiella cybiformis**	*Assipetra terebrodentarius*	*Broinsonia constricta*	*Cretarhabdus ehrenbergii*	*Diazmolithus lehmannii*	*Eiffelithus turriseiffelii*	*Lithraphidites carniolensis*	*Lithastrinus grillii**	*Manivitella pemmatoides*	*Micula clypaeta*	*Microrabdus decoratus**	*Micula decussata**	*Micula murus*	*Nannoconus*	*Prediscosphaera cretacea*	*Prediscosphaera grandis*	*Quadrum svabenickae*	*Retecapsa suriella*	*Rucinolithus magnus*	*Rotelapillius lafitei*	*Tegmentum stradneri*	*Uniplanarius gothicus**	*Uniplanarius sissinghii**	*Watznaueria barnesae*	*Watznaueria biporta*	*Watznaueria britanica*	*Watznaueria fossacincta*	*Watznaueria manivitella*	*Watznaueria sp. (byackii)*	*Zeugrhabdotus embergii*
U1348A-2R-1, 6 cm	84.26	—	F	—	R	C	C	F	C	—	R	—	R	—	—	—	F	F	—	—	—	R	—	F	R	C	—	—	C	—	F	R
U1348A-2R-1, 8 cm	84.28	—	R	—	R	C	C	F	F	—	R	—	R	—	—	—	—	R	R	—	—	—	—	F	—	F	—	—	C	—	F	R
U1348A-2R-1, 10 cm	84.30	—	C	—	R	F	C	—	C	—	F	—	R	—	—	—	R	C	R	—	—	—	—	F	—	C	—	—	C	—	R	F
U1348A-2R-1, 15 cm	84.35	—	C	—	R	C	C	R	—	—	F	—	F	—	—	—	C	C	—	—	—	—	—	F	—	F	—	—	C	C	—	C
U1348A-2R-1, 20 cm	84.40	—	C	—	R	C	R	R	F	—	F	—	F	—	—	—	C	C	R	—	—	—	—	F	—	—	—	F	A	C	—	F
U1348A-2R-1, 25 cm	84.45	—	F	—	R	C	F	R	—	—	R	—	R	R	—	—	C	F	—	—	R	—	—	F	—	C	—	—	C	R	—	R
U1348A-2R-1, 30 cm	84.50	—	C	—	F	C	C	F	—	—	F	—	R	—	—	—	C	C	R	—	—	—	—	C	—	C	—	R	C	C	—	F
U1348A-2R-1, 35 cm	84.55	—	C	—	R	C	F	R	—	—	R	—	F	—	—	R	C	C	R	—	R	—	—	R	—	—	—	—	A	R	—	R
U1348A-2R-1, 40 cm	84.60	—	F	—	R	F	C	R	—	—	F	—	R	—	—	R	C	C	R	—	R	—	—	F	—	F	C	R	C	R	—	R
U1348A-2R-1, 45 cm	84.65	—	F	—	R	F	F	F	—	—	R	—	F	—	—	R	C	C	R	—	—	—	—	F	—	R	—	—	C	R	—	R
U1348A-2R-1, 50 cm	84.70	—	F	—	R	F	F	C	—	—	F	—	R	—	—	R	C	C	—	—	R	—	—	C	—	—	—	—	C	R	—	—
U1348A-2R-1, 55 cm	84.75	—	F	—	R	C	R	C	—	—	F	—	F	—	—	R	C	C	R	—	R	—	—	F	—	—	—	R	C	R	—	—
U1348A-2R-1, 60 cm	84.80	—	R	—	R	C	C	C	—	—	C	—	R	—	—	R	C	F	R	—	R	—	—	C	—	R	—	—	C	C	—	—
U1348A-2R-1, 65 cm	84.85	—	—	—	R	C	F	R	—	—	F	—	F	R	—	R	C	C	—	—	R	—	—	C	—	R	—	—	C	C	—	—
U1348A-2R-1, 70 cm	84.90	—	C	—	R	C	R	F	—	—	F	—	C	—	—	F	C	C	—	—	R	—	—	F	—	F	—	—	C	F	—	F
U1348A-2R-1, 75 cm	84.95	—	F	—	—	C	R	F	—	—	R	—	R	—	—	R	C	C	—	—	—	—	—	R	—	—	R	—	A	R	—	—
U1348A-2R-1, 80 cm	85.00	—	C	—	R	C	R	F	—	—	R	—	R	R	—	C	C	C	—	—	—	—	—	R	—	C	—	—	C	R	—	—
U1348A-2R-1, 85 cm	85.05	R	C	R	R	C	F	C	—	—	F	—	R	—	—	C	C	C	—	—	—	—	—	R	—	—	—	—	A	F	—	F
U1348A-2R-1, 90 cm	85.10	R	C	—	R	F	F	F	—	—	F	—	R	R	—	C	C	C	—	—	R	—	—	R	—	A	—	—	A	F	—	R
U1348A-2R-1, 95 cm	85.15	R	F	—	R	R	R	R	—	—	R	—	F	—	—	F	C	C	—	—	—	R	R	R	—	—	—	—	A	R	—	R
U1348A-2R-1, 100 cm	85.20	—	C	—	—	F	—	F	—	—	R	—	R	—	—	F	C	C	—	—	—	—	R	R	—	R	—	R	A	—	—	F
U1348A-2R-CC, 2 cm	85.29	—	F	R	—	R	R	R	—	R	R	—	R	R	—	R	C	C	—	—	R	—	—	R	—	C	—	—	A	F	—	C
U1348A-2R-CC, 7 cm	85.34	—	—	—	—	R	R	R	—	—	—	—	—	R	—	F	C	C	—	R	R	—	R	—	—	C	—	—	A	C	—	F
U1348A-2R-CC, 11 cm	85.38	—	—	—	—	R	R	R	—	F	F	R	F	—	R	F	C	C	—	F	—	R	R	R	—	—	R	C	C	—	C	C
U1348A-2R-CC, 16 cm	85.43	—	R	R	—	R		R	—	R	R	R	R	—	R	R	C	C	—	C	R	R	—	—	—	—	R	C	C	—	C	C
U1348A-2R-CC, 21 cm	85.48	—	—	F	—	F	F	R	—	F	F	—	R	R	R	F	C	C	—	C	R	—	—	—	—	C	—	—	C	C	A	R

Note: Species with rare occurrence at single sample eliminated from this list (except for *U. sissinghii*)
*Age-diagnostic species listed in Expedition 324 Scientists (2010, Table T2)
A = abundant (>10–100 specimens per field of view)
C = common (>1–10 specimens per field of view)
F = frequent (1 specimen per 1–10 fields of view)
R = rare (<1 specimen per 10 fields of view)
— = absent

TABLE S3. BULK SEDIMENT $CACO_3$, TOC, AND STABLE ISOTOPE DATA, IODP SITE U1348

Sample ID	Depth: mid-point (mbsf)	$CaCO_3$ (wt.%)	TOC (wt.%)	$\delta^{13}C$ (‰ VPDB)	$\delta^{18}O$ (‰ VPDB)	$\delta^{13}C$: duplicate (‰ VPDB)	$\delta^{18}O$: duplicate (‰ VPDB)
U1348A-2R-1, 9–10 cm	84.295	95.845	0.297	2.992	-0.687	—	—
U1348A-2R-1, 20–21 cm	84.405	93.802	0.297	2.915	-0.708	2.898	-0.594
U1348A-2R-1, 30–31 cm	84.505	96.070	0.023	2.918	-0.745	2.806	-0.703
U1348A-2R-1, 40–41 cm	84.605	94.782	0.171	2.958	-0.714	—	—
U1348A-2R-1, 50–51 cm	84.705	96.894	0.006	2.927	-0.547	—	—
U1348A-2R-1, 60–61 cm	84.805	96.305	0.079	2.899	-0.624	—	—
U1348A-2R-1, 70–71 cm	84.905	95.569	0.080	2.826	-0.814	—	—
U1348A-2R-1, 80–81 cm	85.005	93.935	0.269	2.829	-1.124	—	—
U1348A-2R-1, 90–91 cm	85.105	93.472	0.105	2.863	-1.165	—	—
U1348A-2R-1, 100–101 cm	85.205	93.364	0.234	3.016	-1.264	—	—
U1348A-2R-CC, 3–4 cm	85.305	93.478	0.251	2.817	-1.561	—	—
U1348A-2R-CC, 10–11 cm	85.375	94.766	0.091	2.773	-1.735	—	—
U1348A-2R-CC, 13–14 cm	85.405	95.369	0.064	2.725	-1.655	—	—
U1348A-2R-CC, 23–24 cm	85.505	94.838	0.154	2.713	-1.655	—	—
U1348A-2R-CC, 27–30 cm	85.555	96.289	0.016	—	—	—	—

Note: Horizontal bar = No data present

TABLE S4. BENTHIC FORAMINIFERAL STABLE ISOTOPE DATA, IODP SITE U1348

Sample ID	Age*	Depth: mid-point	*Aragonia*		*Oridorsalis*		*Osangularia*		*Paralabamina hillebrandti*		*Sliterella*		*Nuttallides*	
	(Ma)	(mbsf)	$\delta^{13}C$ (‰ VPDB)	$\delta^{18}O$ (‰ VPDB)	$\delta^{13}C$ (‰ VPDB)	$\delta^{18}O$ (‰ VPDB)	$\delta^{13}C$ (‰ VPDB)	$\delta^{18}O$ (‰ VPDB)	$\delta^{13}C$ (‰ VPDB)	$\delta^{18}O$ (‰ VPDB)	$\delta^{13}C$ (‰ VPDB)	$\delta^{18}O$ (‰ VPDB)	$\delta^{13}C$ (‰ VPDB)	$\delta^{18}O$ (‰ VPDB)
U1348A-2R-1, 11–12 cm	72.4	84.315	0.971	0.680	—	—	—	—	1.286	0.214	—	—	1.100	0.254
U1348A-2R-1, 21–22 cm	72.5	84.415	0.920	0.613	—	—	—	—	—	—	1.241	0.196	—	—
U1348A-2R-1, 31–32 cm	72.6	84.515	0.953	0.568	—	—	—	—	1.311	0.160	—	—	1.212	0.311
U1348A-2R-1, 41–42 cm	72.7	84.615	0.956	0.531	0.701	0.647	—	—	1.311	0.174	—	—	—	—
U1348A-2R-1, 51–52 cm	72.8	84.715	0.912	0.525	—	—	—	—	1.331	0.201	1.237	0.137	—	—
U1348A-2R-1, 61–62 cm	72.9	84.815	0.773	0.578	0.522	0.438	—	—	—	—	—	—	—	—
U1348A-2R-1, 71–72 cm	73.0	84.915	—	—	—	—	—	—	1.354	0.066	—	—	—	—
U1348A-2R-1, 81–82 cm	79.4	85.015	1.145	0.196	1.060	0.206	1.404	0.205	—	—	—	—	—	—
U1348A-2R-1, 91–92 cm	80.0	85.115	1.305	0.155	—	—	—	—	—	—	—	—	—	—
U1348A-2R-1, 99–100 cm	80.6	85.195	1.499	0.010	—	—	1.526	0.019	—	—	—	—	—	—
U1348A-2R-CC, 2–3 cm	83.6	85.295	—	—	1.239	-0.336	—	—	—	—	—	—	—	—
U1348A-2R-CC, 9–10 cm	83.8	85.365	1.338	-0.376	—	—	—	—	—	—	—	—	—	—
U1348A-2R-CC, 14–15 cm	84.0	85.415	1.317	-0.280	1.249	-0.297	—	—	—	—	—	—	—	—
U1348A-2R-CC, 22–23 cm	84.2	85.495	1.243	-0.484	1.110	-0.456	—	—	—	—	—	—	—	—

Note: Horizontal bar = No data present

*Proposed numerical ages used in Figure 2, assigned arbitrarily by referring to probable age ranges of Figure 1B

TABLE S5. FORAMINIFERAL SR ISOTOPE DATA, IODP SITE U1348

Sample ID	Depth: mid-point (mbsf)	$^{87}Sr/^{86}Sr$: raw data	$^{87}Sr/^{86}Sr$: calibrated*	Error†
U1348A-2R-1, 7–8 cm	84.275	0.707685	0.707697	± 0.000008
U1348A-2R-1, 18–19 cm	84.385	0.707635	0.707647	± 0.000007
U1348A-2R-1, 27–28 cm	84.475	0.707682	0.707695	± 0.000013
U1348A-2R-1, 39–40 cm	84.595	0.707677	0.707690	± 0.000015
U1348A-2R-1, 62–63 cm	84.825	0.707650	0.707662	± 0.000009
(ditto)	84.825	0.707642	0.707654	± 0.000010
U1348A-2R-1, 71–72 cm	84.915	0.707658	0.707670	± 0.000013
U1348A-2R-1, 80–81 cm	85.005	0.707550	0.707562	± 0.000009
U1348A-2R-1, 87–88 cm	85.075	0.707559	0.707571	± 0.000008
U1348A-2R-1, 93–94 cm	85.135	0.707547	0.707559	± 0.000009
(ditto)	85.135	0.707562	0.707574	± 0.000012
U1348A-2R-1, 101–102 cm	85.215	0.707547	0.707559	± 0.000011
U1348A-2R-CC, 3–4 cm	85.305	0.707473	0.707485	± 0.000010
U1348A-2R-CC, 10–11 cm	85.375	0.707459	0.707471	± 0.000010
U1348A-2R-CC, 17–18 cm	85.445	0.707485	0.707497	± 0.000010

*Calibrated with respect to NIST SRM 987 = 0.710250

†2 standard error of internal precision